

## **General Disclaimer**

### **One or more of the Following Statements may affect this Document**

- This document has been reproduced from the best copy furnished by the organizational source. It is being released in the interest of making available as much information as possible.
- This document may contain data, which exceeds the sheet parameters. It was furnished in this condition by the organizational source and is the best copy available.
- This document may contain tone-on-tone or color graphs, charts and/or pictures, which have been reproduced in black and white.
- This document is paginated as submitted by the original source.
- Portions of this document are not fully legible due to the historical nature of some of the material. However, it is the best reproduction available from the original submission.

NASA Technical Memorandum 79151

(NASA-TM-79151) METAL-DIELECTRIC  
INTERACTIONS (NASA) 24 p HC A02/MP A01  
CSCL 11F

N79-25195

Unclas  
G3/26 22275

METAL-DIELECTRIC INTERACTIONS

Donald H. Buckley  
Lewis Research Center  
Cleveland, Ohio



Prepared for the  
Conference on Electrical Insulation and Dielectric Phenomena  
sponsored by the National Research Council  
Whitehaven, Pennsylvania, October 21-25, 1979

## INTRODUCTION

There are a wide variety of situations wherein metals are in solid state contact with dielectric materials. Tribological applications are examples. The adhesion, friction, and wear of metals contacting glasses, polymers, ceramics as well as the interface formed for coatings of these materials on metal surfaces find application in many practical tribological devices.

The surfaces of the metal and the dielectric, their structure, physics, chemistry, and mechanics effect the nature of interfacial interactions when the solids are brought into contact. Adsorbates, oxides on the metal, crystallography of both metals and crystalline dielectrics, and the nature of environmental constituents effect interfacial behavior.

The objective of the present paper is to review some of those factors which influence solid state interactions for metals in contact with dielectric surfaces. Since surfaces play such an important part in these interactions the use of analytical tools in characterizing surfaces will be discussed. Adhesion, friction, and wear will be used as indicators of the nature of the bond strength of the metals to the dielectrics.

## RESULTS AND DISCUSSION

### Metal-Dielectric Contacts

Metals contacting glasses. - Where an argon ion sputter cleaned metal surface is brought into contact with an ordinary glass surface which has been heated in vacuum to remove adsorbates and subsequently cooled prior to the solid state contact strong bonds of adhesion develop between the clean metal and the glass. Any attempt at tangential movement of the metal along the glass surface results in fracture in the glass. Subsequent examination of the metal surface reveals the presence of the glass in the metal interfacial region.

In figure 1 friction force (the resistance to tangential movement of the metal along the glass surface) is plotted as a function of the load or force with

which the metal is pressed against the glass surface. The curve presented in figure 1 represents data obtained for three different metals, gold, iron, and aluminum in contact with the same glass surface. A single curve can represent the data for all three metals (ref. 8).

The three metals were selected because of their differences in affinity for the elemental constituents in the glass, gold being the least active and aluminum the most. Glass was found adhered to the clean metal in each case.

Since the friction force in figure 1 is the force required to fracture the glass, and that is essentially unchanged the nature of the metal has little effect. The presence of the glass on the metal surface indicates that the cohesive fracture strength in the amorphous glass is less than the interfacial bond strength between the metal and the glass. If this were not so, then the clean surfaces would separate at the interface.

If the experiments of figure 1 are repeated in moist air with a thin lubricating film of octane, to exclude, to some extent the environment from the interface, entirely different results are obtained. These are presented for gold and iron in contact with glass in figure 2.

The friction force, or force to move the iron tangentially on the glass surface is appreciably less than that observed in figure 1. Adsorption of the octane to previously cleaned metal and glass surfaces reduces markedly interfacial bond strength thereby promoting greater ease of tangential motion.

The friction force in figure 2 for the gold contacting glass is greater at the higher loads than it is for iron. Gold unlike the iron, does not strongly adsorb the octane and the film at the interface can be more easily broken down. As the load is increased the amount of metal in real contact with the glass increases. At 1000 gram load, the friction force has increased to near that observed for the clean surfaces indicating that the lubricating or shielding effectiveness of the liquid has been nearly eliminated.

The importance of environment upon interfacial behavior for metals in contact with dielectrics can readily be demonstrated. Octane, which was used as a blanketing fluid on the surface of the glass in figure 2 has a relatively high vapor pressure. If flowing air is passed over the glass surface containing the octane the vapor is carried away and the moist air interacts with the surface. When this occurs there is a noticeable decrease in the coefficient of friction for the two surfaces in contact. In figure 3, segment A of the friction trace represents the weaker interfacial bonding that occurs between the metal, gold, and the glass surface when the surfaces contact in the presence of moist air. The moment octane is placed on the surface the interfacial bond strength increases and so does the friction. This is reflected in segments B of the actual friction trace presented in figure 3. The data of figure 3 indicate the importance of environment on the interfacial interaction of a metal with a dielectric surface.

With metals in contact with glass surfaces in vacuum, as has already been discussed, the interfacial bond strength is such that fracture occurs in the glass. Where the glass surface is exposed to moisture as in figures 2 and 3 metal transfers to glass. This observation has been made by other investigators as well (ref. 1).

The application of an effective boundary lubricant such as an organic acid to a glass surface reduces appreciably the bond strength between a metal and the glass by preventing solid state interfacial contact of the solids. The presence of such a film can nearly completely eliminate fracture in the glass and shear in the metal. The reason for this is that the weakest bonding at the interface exists between the acid molecules adsorbed to both surfaces. The nature of the metal contacting the glass is therefore of lesser importance. This is indicated in the data of figure 4.

Stearic acid is an effective boundary lubricant and in figure 4 very little difference is observed in friction behavior between gold and iron in contact with

glass. Because, however, the acid now plays such a strong role in interfacial behavior its properties become extremely important. The importance of these properties was recognized very early (ref. 3).

#### Crystalline Oxides Contacting Metals

When crystalline oxides contact metal surfaces the nature of interfacial bonds that develop depend very heavily upon the orientation of the oxide at the interface. This has been observed in the adhesion, friction, and wear behavior of these materials (refs. 4 to 8).

In addition to the orientation of the oxide, the metal orientation is extremely important. This is demonstrated in the data of figure 5. A tungsten disk with very large grains was analyzed to determine the orientation of each grain at the surface. The orientations are depicted in the drawing under the disk photograph of figure 5(a) and in the unit triangle of figure 5(b). A fixed orientation of sapphire  $(10\bar{1}0)[000\bar{1}]$  was slid on the tungsten disk very slowly out near the circumferential edge (dashed line in fig. 5(a)). The friction force, a measure of the interfacial bond strength, was measured for each point along the disk surface. This was done in both vacuum and air. The friction coefficients obtained are presented in figures 5(c) and (d).

The results of figure 5 indicate that not only does the crystallographic plane effect interfacial behavior but changes in direction within a particular grain can produce very pronounced effects. Further, as has already been observed environment produces dramatic changes in friction behavior which reflects the changes in interfacial bond strength.

It is of interest to note in figure 5 that not only is friction generally less in air but the relative amount of the reduction is strongly a function of direction in any grain. One might anticipate differences in adsorbate uptake for a given exposure to air for the various grain orientations present on the disk surface and, accordingly, differences in interfacial bond strengths and friction force. The variation with direction is, however, somewhat more surprising.

### Metal-Carbide Interactions

Silicon carbide is one of the most widely used grinding materials. It is most frequently used in the removal of metal. There is solid state interfacial contact between the dielectric and the metal. The nature of interfacial bonding effects the life of the silicon carbide. If strong interfacial adhesive bonding occurs metal can transfer to the silicon carbide surface or fracture can occur in the silicon carbide. Either event is detrimental.

The interfacial bonding of metals to silicon carbide is extremely sensitive to the nature and composition of the surface. Variations in the nature of the carbide surface chemistry can alter interfacial bonding and in turn friction forces for metals contacting that surface.

Figure 6 contains friction data for titanium metal in contact with silicon carbide in various states, sputter cleaned, with an ion bombarded oxygen film and with a simple adsorbed film of oxygen present. With the initial sliding across the surface difference in friction behavior exist indicating differences in interfacial bond strengths. Repeated passes over the same surface results in the generation of a new surface which, ultimately after 10 passes is nearly identical and this is reflected in the friction data of figure 6.

Not only do binding properties of the dielectric but those of the metal will have an influence on the interfacial bond strength for metals in contact with materials such as silicon carbide. For example, with transition metals, the chemical activity of the metal as reflected in the percent of a valence (d) bond character effect the interfacial bond strength. The more chemically active the metal (i.e., the smaller the percent d-bond) the stronger the bond and the higher the friction coefficient (ref. 9). This is demonstrated in the data of figure 7 for various transition metals in contact with silicon carbide.

### Polymer-Metal Interactions

In our laboratory we have for some time been studying polymer-metal interactions using both Auger emission spectroscopy and field ion microscopy (ref. 10). The field ion microscopic used in conjunction with the atom probe can give detailed structural and chemical information at the atomic level. Each individual surface atom site can be identified and the chemistry of a single atom fingerprinted.

Figure 8 is a field ion photomicrograph of a tungsten surface. Each individual white spot indicating an individual atomic site and the rings representing atomic planes. Incorporated directly into the field ion microscope is an adhesion device. The details of it and other analytical tools used in adhesion experiments are reviewed in reference 11.

Polyimide is an extremely promising polymer for potential use in tribological applications. Its wear behavior is, however, highly sensitive to the nature of the interface when in contact with metals. This is related to interfacial adhesion of the polymer to the metal surface. Detailed field ion microscopy studies of the adhesion of polyimide to metal surfaces have therefore been conducted. A photomicrograph of a tungsten surface after contact is presented in figure 9.

An examination of figure 9 indicates that the tungsten metal surface atoms seen in figure 8 have been completely covered by polyimide (PI in figure) which have transferred to the metal surface as a result of solid state contact. The interfacial adhesion forces between the metal and polymer are stronger than the cohesive forces in the polymer. This has been consistently observed with other dissimilar materials in contact as well. The interfacial bond is generally stronger than the cohesive bond in the cohesively weaker of the two materials (ref. 11).



If the normal force applied to the polymer in contact with the metal is increased, the amount of polymer transferred to the metal surface also increases. In figure 10 the polymer transfer film appears as rod-like structures present on the surface. These are larger polymer fragments than observed in figure 9 at lighter normal forces. Field evaporation of the polymer from the metal surface indicates that the chain-like fragments of figure 10 extend further above the metal surface than those of figure 9. With continued field evaporation the polymer film can ultimately be completely stripped away leaving the clean tungsten. Similar observations have been made with other polymers such as polytetrafluoroethylene (ref. 10).

#### INTERFACIAL OXIDE FILMS

Many applications exist for the use of refractory compounds. Application areas include the field of tribology. The interface between the coating and substrate is extremely important, as is its characterization. In tribological applications there is yet another interface, that existing between the refractory compound coating and a metal or alloy surface in sliding or rolling contact with the free surface of the refractory compound coating. This is depicted schematically in figure 11.

In figure 11 a 440C bearing steel substrate is indicated as having a coating on its surface. A steel pin is in sliding contact with the coated surface. When a load is applied to the steel pin and it moves tangentially across the surface cracks can develop in the coating. Adhesion of the coating to the substrate is extremely important. If adhesion between coating and metal substrate is poor the coating can spall off at the surface leaving substrate metal exposed as indicated in figure 11. With subsequent passes of the steel pin across the surface steel can transfer to the exposed substrate and this transferred metal will, when deformed by the steel pin, cause the spallation of more coating material.

It becomes fairly obvious from the foregoing discussion that whatever can be done to improve interfacial adhesion will benefit coating life and performance. During the course of our studies it has been found that the presence of oxide films on the metal surface improves adhesion. This oxide layer can be developed by oxidation of the metal or alloy substrate prior to deposition of the refractory compound. If the substrate shown in figure 11, for example, is oxidized the Auger emission spectrum for that can be used as an indicator of oxygen uptake on the surface.

Figure 12 is an Auger spectrum for the 440C surface that has been oxidized. The spectrum indicates the major metallic elements present namely, iron, chromium, carbon, and oxygen. The carbon can arise from two sources, the carbide present in the alloy and adsorbed gases of carbon monoxide and carbon dioxide which may be present on the surface.

While Auger emission spectroscopy analysis is extremely useful in identifying the elements present on the surface and can give some indication of compound formation from chemical shifts, x-ray photoelectron spectroscopy (XPS) is more effective in fingerprinting surface compounds. An XPS spectrum for the  $1s$  oxygen spectral line from the 440C surface analyzed with Auger in figure 12 is presented in figure 13. The source of the oxygen of figure 12 can be seen in figure 13 where the binding energies for oxygen, adsorbed oxygen, and oxides have been sorted out with the aid of an analog curve resolver. In addition to adsorbed oxygen, chromium oxide ( $\text{Cr}_2\text{O}_3$ ) and two oxides of iron  $\text{Fe}_2\text{O}_3$  and  $\text{FeO}$  appear to be present. Thus, with XPS the source of oxygen can be pinpointed.

When a refractory compound such as molybdenum disilicide or molybdenum boride is initially sputter deposited on the 440C surface containing the oxide film a coating of mixed chemistry results. With the silicide at the oxide refractory compound interface both molybdenum disilicide and silicon dioxide ( $\text{SiO}_2$ ) are present as indicated in the XPS data of figure 14(a). The deposition of the boride

in its early stages results in both molybdenum boride and boric oxide being present at the interface (fig. 14(b)). If coating deposition continues ultimately only the refractory compound is detected.

The composition, amount and depth of oxide between metal substrate and refractory compound is altered by the amount of surface oxidation that takes place as well as other parameters such as biasing or not biasing the metal substrate. A refractory carbide coating of  $\text{Mo}_2\text{C}$  was sputter deposited onto a 440C substrate under various conditions, no biasing, biasing the substrate at -300 volts and with oxidation. Depth profile analysis of the refractory coating, the oxide and the substrate surfacial layers was conducted. The results obtained are presented in figure 15.

It is interesting to note in figure 15 the differences in composition for the three cases also that the iron oxide of figure 12 which was  $\text{Fe}_2\text{O}_3$  has been reduced to the lower oxide of iron  $\text{Fe}_3\text{O}_4$ . In all likelihood the oxygen is consumed in the conversion of some of the carbide to oxide.

When the surface oxides were removed from the 440C steel surface as in figures 15(a) and (b) the adhesion of the refractory compound to the substrate was extremely poor. It just peeled away from the surface. The oxide interlayer sandwiched between the metal and the refractory compound appeared to be necessary.

In an attempt to understand which of the two elemental metallic components of the substrate indicated in figure 12 was responsible, if either, for the poor adherence sputter etched clean iron and chromium surfaces were sputter coated with molybdenum carbide. Photomicrographs of these two surfaces are presented in figures 16(a) and (b). The coating on the iron surface remained fully in tact while that on the chromium surface peeled and flaked off the surface.

Preoxidation of the iron surface to form  $\text{Fe}_2\text{O}_3$  improved adhesion but also altered the morphology of the surface film (see fig. 16(c)).

If the oxidized 440C containing  $\text{Fe}_2\text{O}_3$  is coated with molybdenum, carbide, boride, or silicide by radiofrequency sputtering the interfacial region will contain varied oxides. Figure 17 is a schematic representation of the interfacial region with these three coating materials on a 440C substrate as determined from ion profiling with XPS analysis through the film to the interfacial region and then on to the substrate.

The first most general observation to be made is that the  $\text{Fe}_2\text{O}_3$  and FeO formally present on the 440C have been replaced by  $\text{Fe}_3\text{O}_4$  with all three films. Next with the molybdenum carbide in addition to iron oxide, molybdenum oxide ( $\text{MoO}_2$ ) is present in the iron oxide and molybdenum carbide.

With both molybdenum boride and molybdenum silicide in figure 17 two oxides in addition to iron oxide are present in the interfacial region. Just as with the carbide film the oxide of molybdenum ( $\text{MoO}_2$ ) is present at the interface. In addition to these with the boride there is boric oxide ( $\text{B}_2\text{O}_3$ ) and with the silicide there is silicon dioxide ( $\text{SiO}_2$ ). The presence of the oxides in the interface region help to promote strong adhesion of the refractory compound to the substrate.

The friction and wear behavior of coatings are a good indicator of the adhesion of the coating to the substrate. If adhesion is good the coating will exhibit its characteristic friction properties. Further, since the basic coating material has inherently good wear resistance, if it remains adhered to the surface wear should also be low. The data of figure 18 indicates the friction and wear performance of the molybdenum boride, molybdenum silicide, and the molybdenum carbide for the oxidized surface. The data indicate that the molybdenum carbide imparts the lowest friction and wear to the surface.

## SUMMARY REMARKS

The nature of interfacial bonding between metals and dielectrics can be effectively determined with adhesion and friction force measurements. Films present on the surface such as oxygen or water vapor markedly alter adhesive bond strengths which in turn affects friction force and interfacial fracture when attempts are made to separate the regions of contact. Metal-to-dielectric contacts are sensitive to the metal surface orientations with adhesion and friction force varying with orientation.

Analytical surface tools such as the field ion microscope, Auger emission spectroscopy and x-ray photoelectron spectroscopy are very effective in providing insight in the effect of contact on the surfaces of metal and dielectrics. They indicate the region of interfacial separation for metal-to-polymer contacts and when the spectroscopy devices are used with ion depth profiling they provide information on the role of surface oxides in the adhesion of coatings to metal surfaces.

## REFERENCES

1. F. P. Bowden and D. Tabor, *The Friction and Lubrication of Solids*, Pt. I, Oxford Press (1950).
2. S. M. Wiederhorn, *Environment-Sensitive Mechanical Behavior of Materials*, Gordon and Breach, 293 (1966).
3. W. B. Hardy, *Collected Scientific Papers*, Cambridge Press (1936).
4. R. P. Steijn, *J. Appl. Phys.*, 32[10] 1951 (1961).
5. E. J. Duwell, *ASLE Trans.*, 12, 34 (1969).
6. D. H. Buckley, NASA TN D-5689 (1970).
7. K. F. Dufrane and W. A. Glaeser, NASA CR-72295 (1967).
8. D. H. Buckley, *Friction, Wear, and Lubrication in Vacuum*, NASA SP-277 (1971).
9. K. Miyoshi and D. H. Buckley, NASA TN.

10. W. A. Brainard and D. H. Buckley, NASA TN 6524 (1971).
11. D. H. Buckley, *Wear*, 46, 19 (1978).
12. D. R. Wheeler, NASA TM 788139 (1978).
13. D. R. Wheeler and W. A. Brainard, NASA TP-1161 (1978).
14. W. A. Brainard and D. R. Wheeler, NASA TP-1156 (1978).
15. W. A. Brainard and D. R. Wheeler, *J. Vac. Sci. Technol.* 15 (6) 1800 (1978).

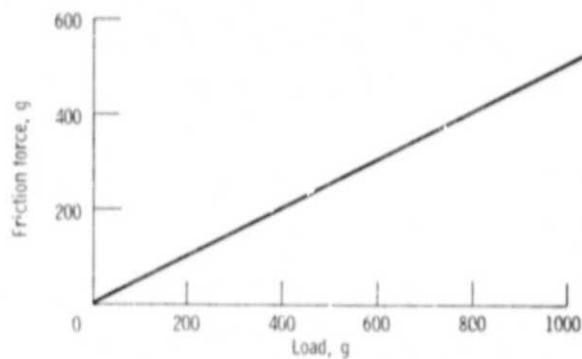


Figure 1. - Friction force as function of load for gold, iron or aluminum sliding on glass. Vacuum; sliding velocity, 30 centimeters per minute; temperature  $23^{\circ}\text{C}$ .

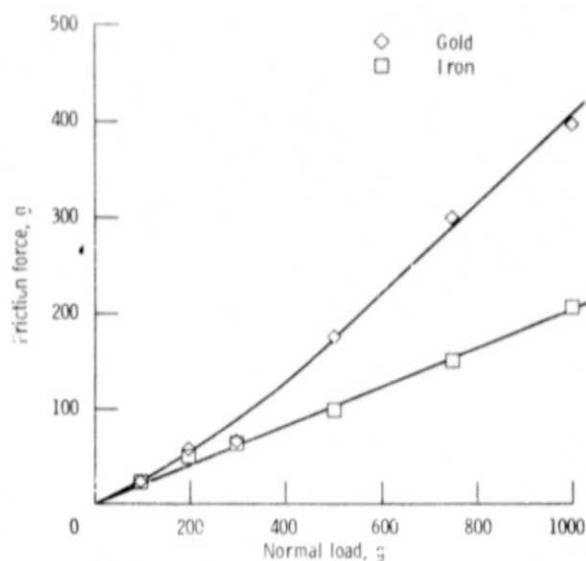


Figure 2. - Friction force at various normal loads for gold and iron sliding on glass lubrication with thin film of octane. Moist air; sliding velocity, 30 centimeters per minute; temperature,  $23^{\circ}\text{C}$ .

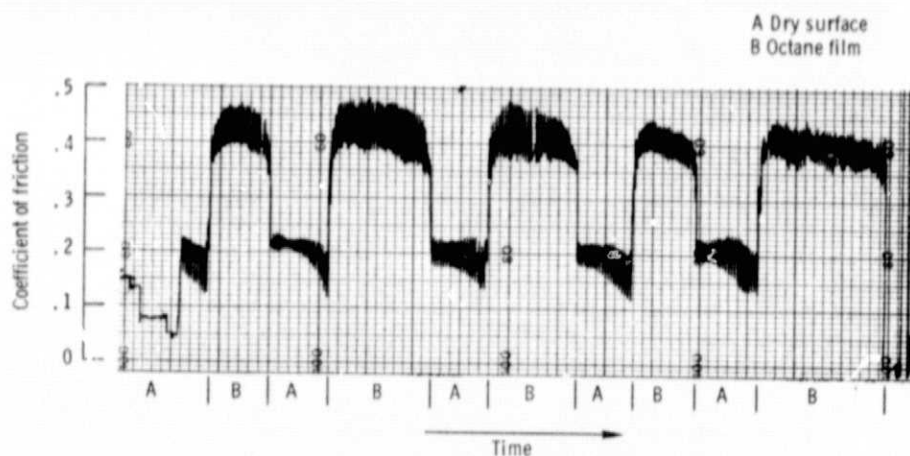


Figure 3. - Coefficient of friction for gold sliding on glass with and without octane film. Moist air; sliding velocity, 30 centimeters per minute; load, 100 grams; temperature, 23° C.

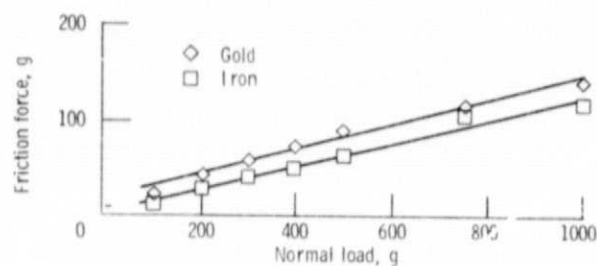
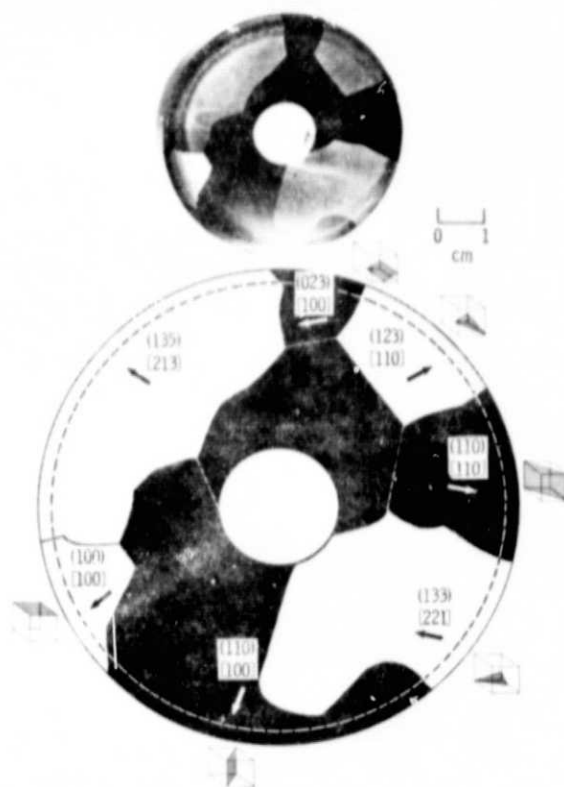


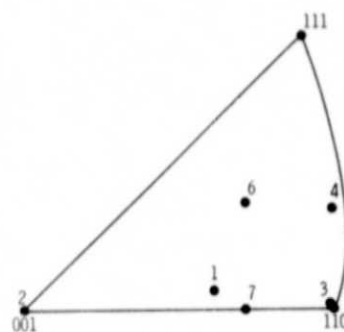
Figure 4. - Friction force as function of normal load for gold and iron sliding on glass lubricated with 0.20 percent stearic acid in hexadecane. Sliding velocity, 30 centimeters per minute; temperature, 23° C.



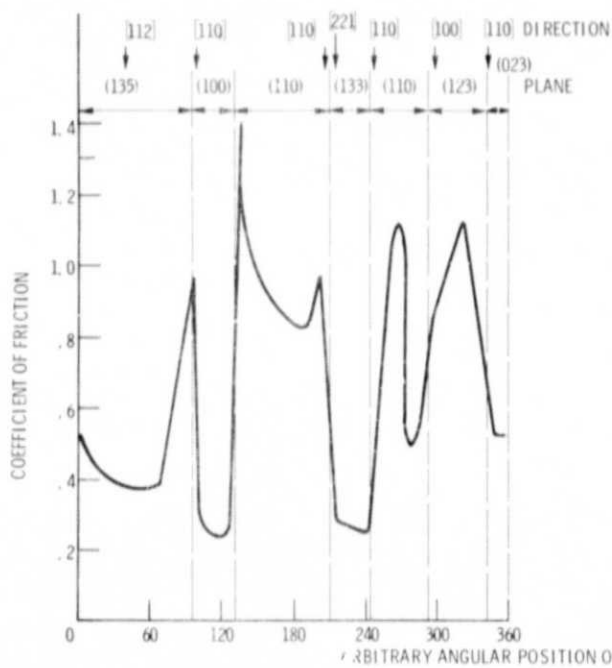
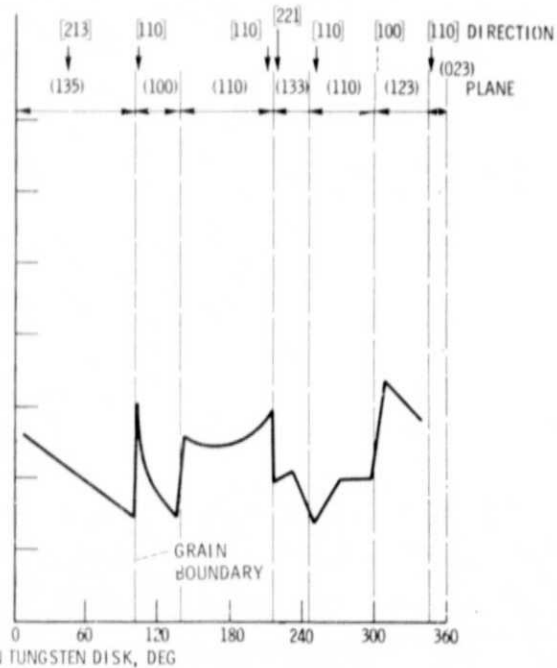


CD-8131

(a) TUNGSTEN DISK



(b) UNIT TRIANGLE.

(c) IN VACUUM ( $10^{-10}$  MM Hg).

(d) IN AIR (760 MM Hg).

Figure 5. - Coefficient of friction of sapphire  $(10\bar{1}0)$  plane sliding  $[0001]$  direction on polycrystalline tungsten. Load, 500 g; sliding velocity, 0.013 cm/sec.

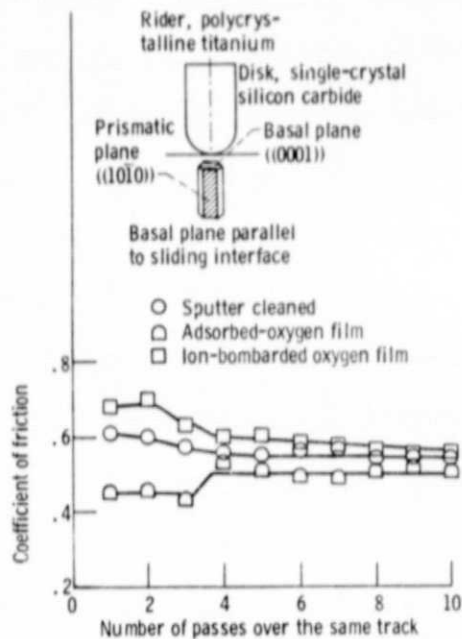


Figure 6. - Average coefficients of friction for titanium rider and silicon carbide disk sets (1) with adsorbed-oxygen film and (2) with ion-bombarded oxygen film.

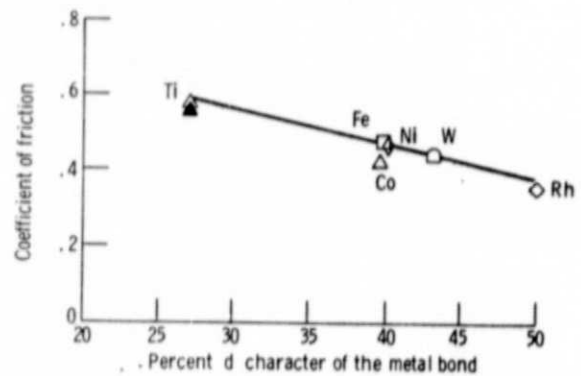


Figure 7. - Coefficient of friction as function of percent of metal d bond character for single-crystal silicon carbide (0001) surface in sliding contact with various metals in vacuum ( $10^{-8}$  N/m<sup>2</sup>). Sliding direction,  $\langle 10\bar{1}0 \rangle$ ; sliding velocity, 3 mm/min; load, 5 to 50 grams; temperature, 25°C.

ORIGINAL PAGE  
OF POOR QUALITY



Figure 8. - Tungsten prior to contact (15.0 kV, helium image gas, liquid nitrogen cooling).

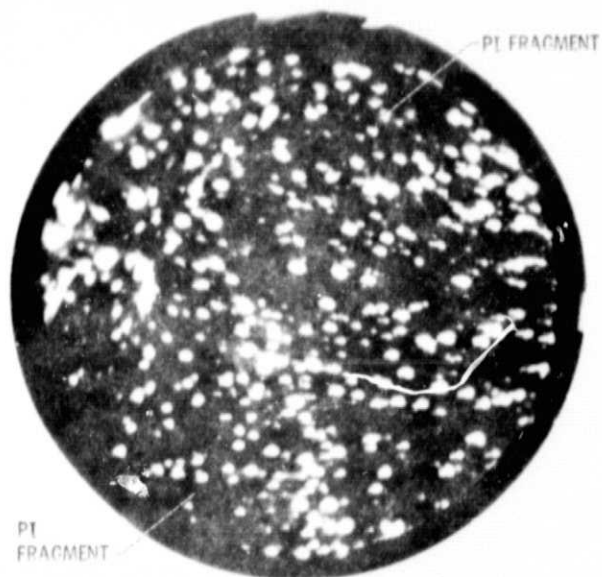


Figure 9. - Tungsten after polymide contact (13.0 kV, helium image gas, liquid helium cooling).

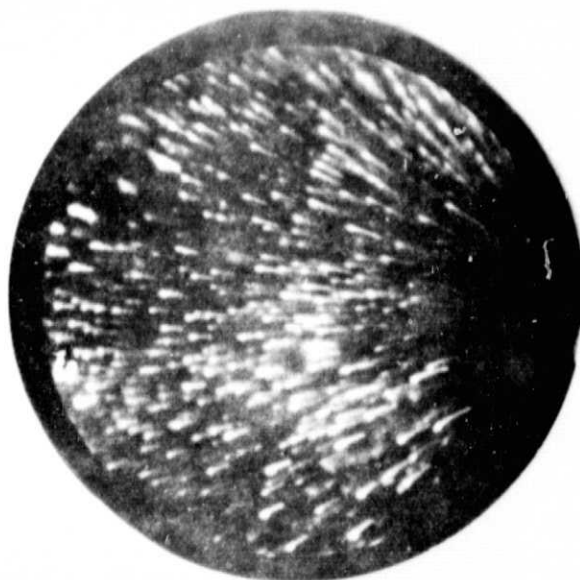


Figure 10. - Tungsten after polymide contact (9.25 kV, helium image gas, liquid helium cooling).

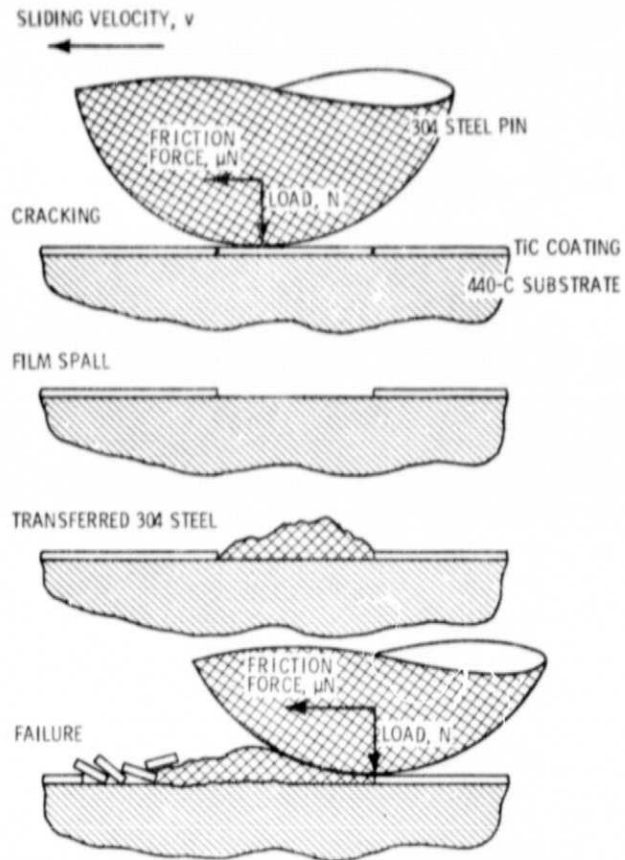


Figure 11. - Schematic illustration of progressive coating failure for steel pin sliding on RF sputtered coating on 440-C disk.

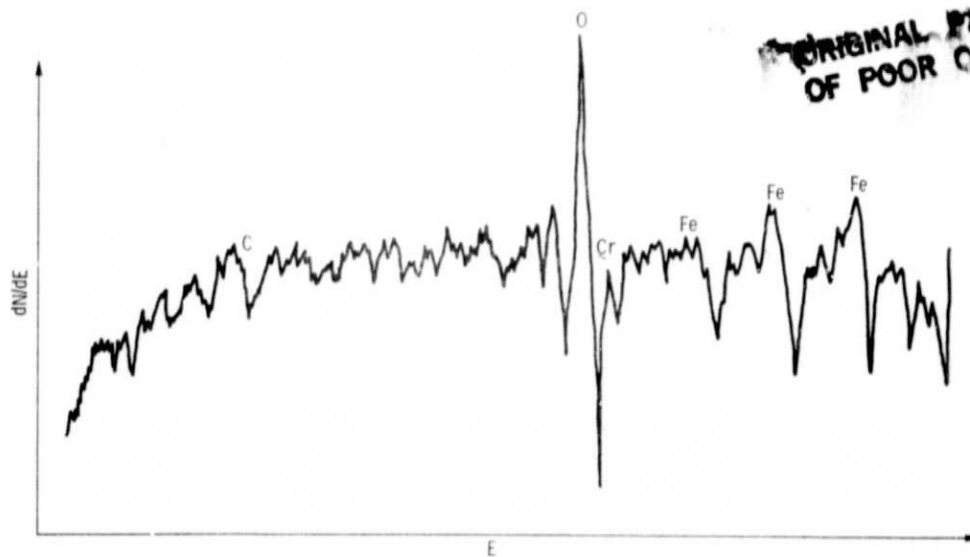


Figure 12. - Auger spectrum of oxidized 440C steel disk. Furnace temperature,  $340^{\circ}\text{C}$ ; duration, 20 hr.

ORIGINAL PAGE IS  
OF POOR QUALITY

ORIGINAL PAGE IS  
OF POOR QUALITY

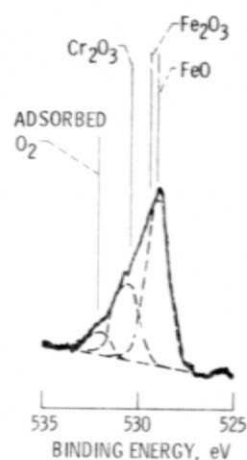
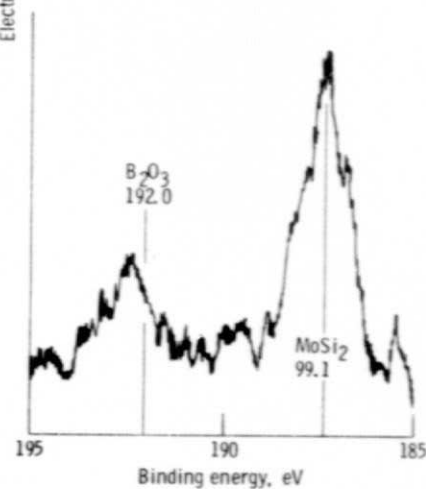
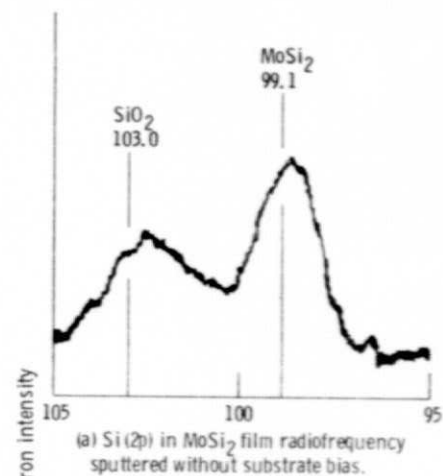
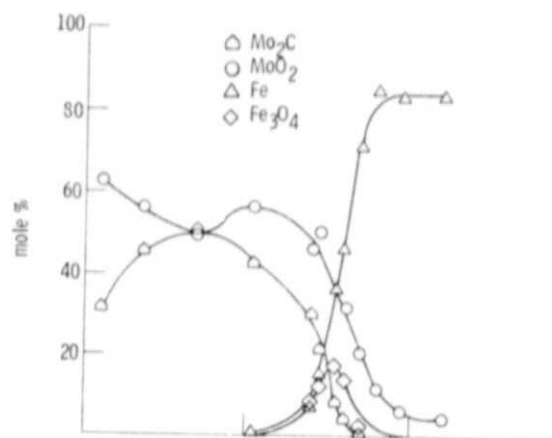


Figure 13. - Oxygen (1s) spectral line from wear test specimen showing binding energies of 1s electron in several compounds and resolution of peak obtained with analog curve resolver (ref. 14).

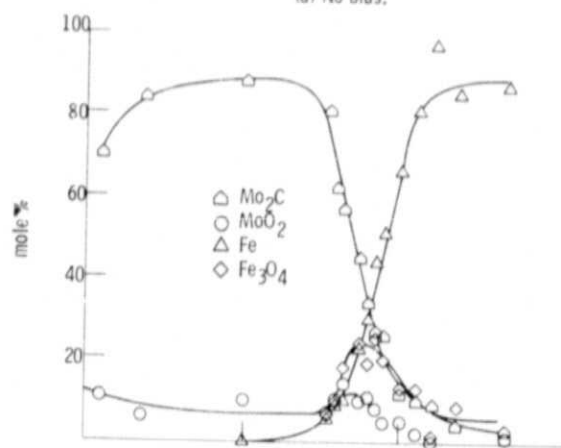


(b) B (1s) in  $\text{Mo}_2\text{B}_5$  film radiofrequency sputtered with -300-volt substrate bias.

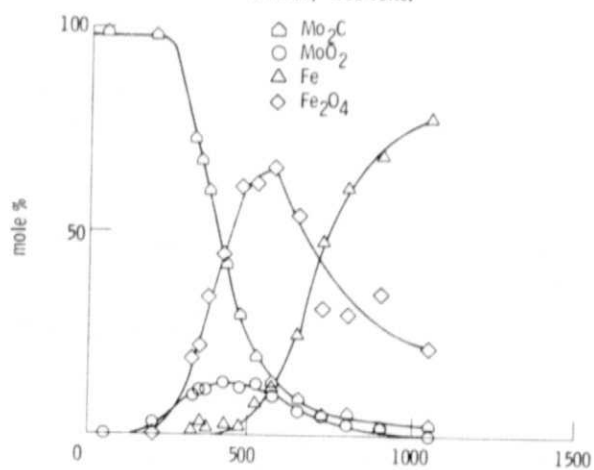
Figure 14. - X-ray photoelectron spectroscopy peaks showing separation of peak due to oxides from that due to molybdenum compound.



(a) No bias.

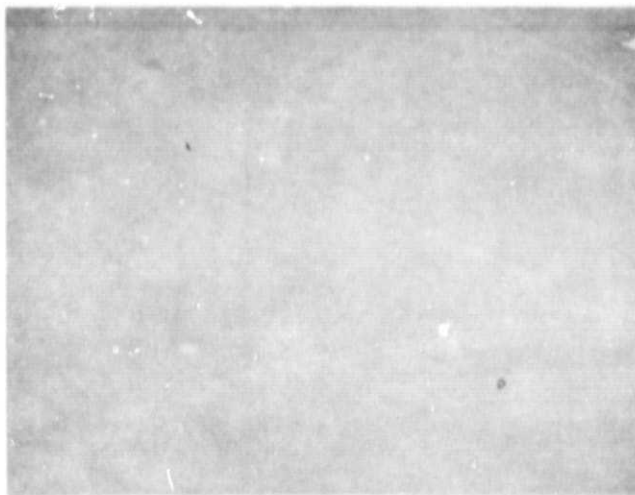


(b) Bias, -300 volts.

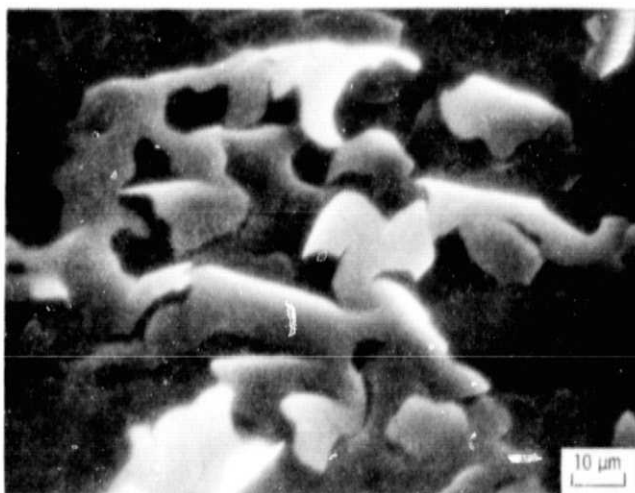


(c) Oxidized 440C substrate. Bias, -300 volts.

Figure 15. - Depth profile of sputtered  $\text{Mo}_2\text{C}$  films (ref. 13).

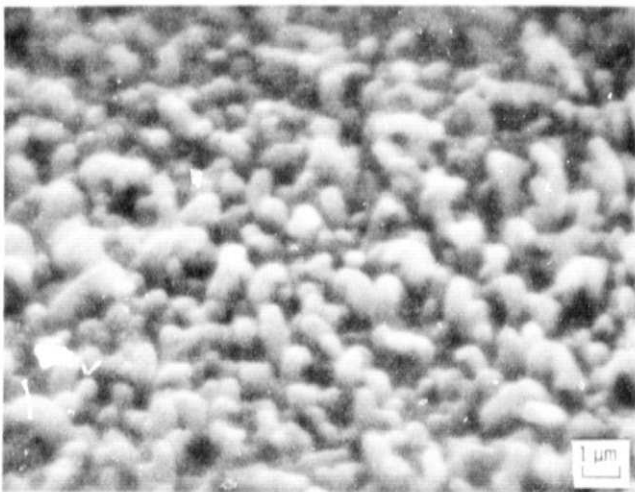


(a) IRON.

ORIGINAL PAGE IS  
OF POOR QUALITY

(b) CHROMIUM.

Figure 16. - Iron and chromium radiofrequency splitter coated with molybdenum carbide with a -300 volt bias.



(c) PREOXIDIZED IRON.

Figure 16. - Concluded.

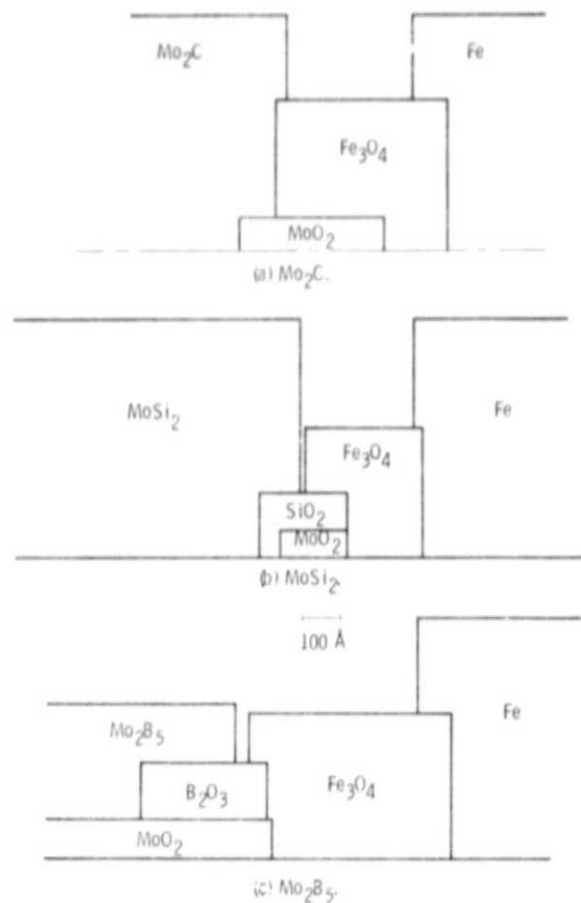


Figure 17. - Schematic representation of interfacial region of  $\text{Mo}_2\text{C}$ ,  $\text{MoSi}_2$ , and  $\text{Mo}_2\text{B}_5$  radiofrequency-sputter coatings on oxidized 440C substrates. Bias, -300 volts (ref. 12).

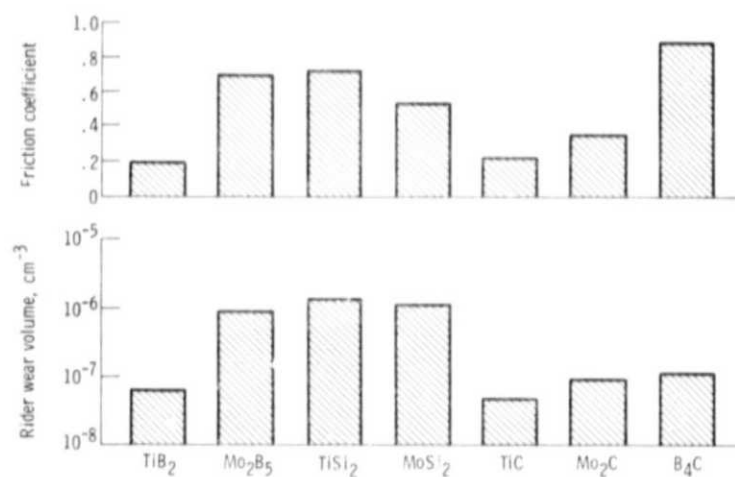


Figure 18. - Friction coefficient and rider wear after running on various rf sputtered coatings on 440-C disk, load 0.25 N, speed  $25 \text{ cm s}^{-1}$ , nitrogen atmosphered, duration 30 min, disk oxidized.